

Effects of Plasma Rotation on Interchange Modes in LHD

市口勝治^{1,2)}, 鈴木康浩^{1,2)}, 佐藤雅彦¹⁾, 藤堂泰^{1,2)}, T. Nicolas¹⁾,
B.A.Carreras³⁾, 榊原悟^{1,2)}, 武村勇樹¹⁾, 大館暁^{1,2)}, 成嶋吉朗^{1,2)}

核融合研¹⁾、総研大²⁾、Universidad Carlos III, Spain³⁾

第21回NEXT研究会,
京都テルサ, 2016年3月10日—3月11日

Acknowledgements

This work is supported by the budget NIFS15KNST077 of National Institute for Fusion Science, and JSPS KAKENHI 15K06651. Plasma simulator (NIFS) and Helios(IFERC-CSC) were utilized for the calculations.



1. Motivation

LHD experimental data for plasma rotation

2. Numerical method of 3D MHD simulation

Procedure of the analysis

Flow model

3. Simulation results with finite flow

Magnetic configuration and equilibrium results

Time evolution of pressure driven mode

Flow effects on linear modes

Flow dependence of nonlinear dynamics

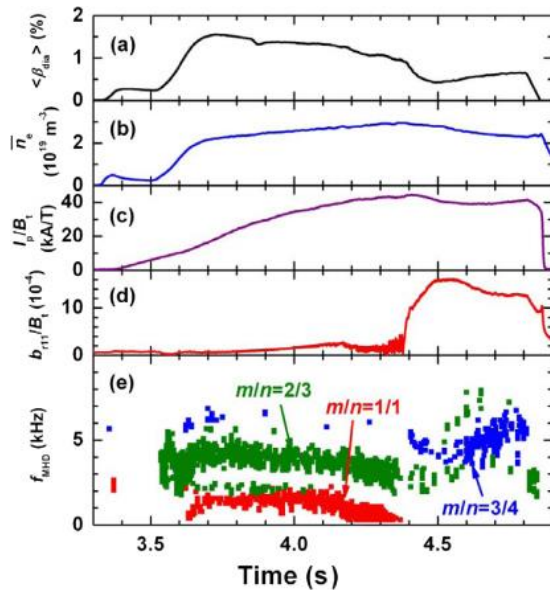
4. Summary & Future Plan

- Observation of flow and partial collapse in LHD experiments

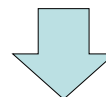
Rotation stop & collapse

Sakakibara et al., NF (2013) 043010 .

Rax=3.6m, $\gamma_c=1.18$, $\langle\beta_{dia}\rangle\sim 1.5\%$



When the rotation of $m=1/n=1$ mode stops, the mode abruptly grows and beta value drops.

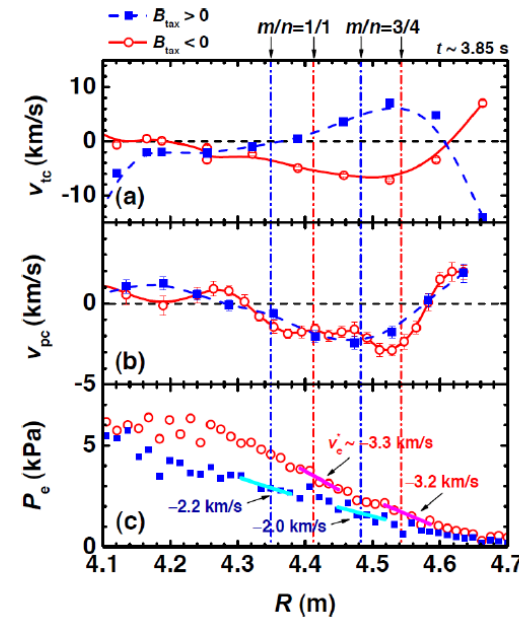


- The rotation may suppress the mode growth.

Typical carbon flow in LHD

Y.Takemura et al., PFR (2013) 140123 .

Rax=3.6m, $\gamma_c=1.254$, $\langle\beta_{dia}\rangle\sim 1.5\%$



Maximum poloidal carbon flow is a few km/s.

- ◆ We would like to study the effects of global shear flow on the stability of interchange modes in a Large Helical Device (LHD). by utilizing **3D** numerical equilibrium and dynamics codes.
- ◆ However, a 3D equilibrium calculation scheme consistent with global flow has not been established for heliotrons.
- ◆ **Static equilibrium is employed and a model poloidal flow is incorporated as the initial perturbation of the dynamics calculation.**
- ◆ The **HINT2** code (Y.Suzuki, et al. NF(2006)L19) is utilized for the 3D static equilibrium calculation.
The HINT2 code solves the 3D equilibrium equations without any assumptions of the existence of the nested flux surfaces
- ◆ The **MIPS** code (Y.Todo, et al. PFR(2010)S2062) is utilized for the 3D dynamics calculation.
The MIPS code solves the full MHD equations by following the time evolution with the HINT2 solution in (R, ϕ, Z) coordinates

◆ Flow model

Coordinate transform between cylindrical and flux coordinates

$$(R, \phi, Z) \iff (\rho, \theta, \phi)$$

Assumptions :

$$\mathbf{V} \cdot \nabla P_{eq}(\rho) = 0 \quad V_\theta^2 = V_R^2 + V_Z^2$$

$$V_R = \frac{1}{A^2} \left[-\frac{1}{R} \frac{\partial P_{eq}}{\partial \phi} \frac{\partial P_{eq}}{\partial R} V_\phi \pm K \frac{\partial P_{eq}}{\partial Z} \right]$$

$$A^2 = \left(\frac{\partial P_{eq}}{\partial R} \right)^2 + \left(\frac{\partial P_{eq}}{\partial Z} \right)^2$$

$$V_Z = \frac{1}{A^2} \left[-\frac{1}{R} \frac{\partial P_{eq}}{\partial \phi} \frac{\partial P_{eq}}{\partial Z} V_\phi \mp K \frac{\partial P_{eq}}{\partial R} \right]$$

$$K = \left[A^2 V_\theta^2 - \left(\frac{V_\phi}{R} \frac{\partial P_{eq}}{\partial \phi} \right)^2 \right]^{1/2}$$

Focus on poloidal flow : $V_\phi = 0$ and $V_\theta = V_\theta(\rho)$

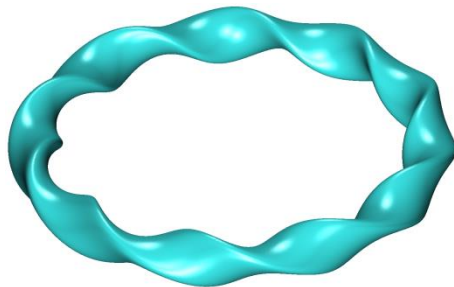
◆ Magnetic configuration

$R_{ax}=3.6m$, $\gamma_c=1.13$, $\beta_0=4.4\%$
no net toroidal current constraint

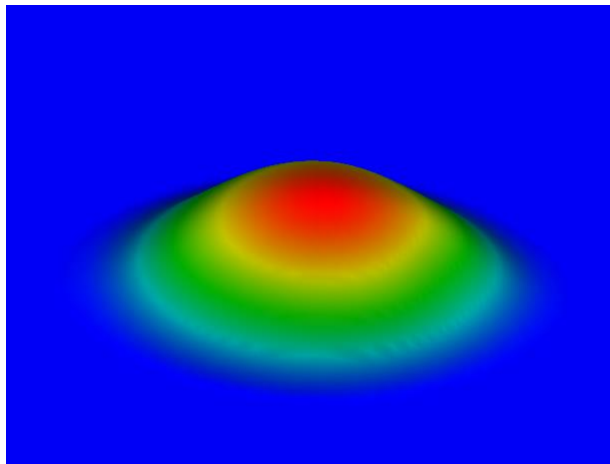
◆ Equilibrium results with model profiles of pressure and flow

$$P_{eq} = P_0(1 - \rho^2)(1 - \rho^8)$$

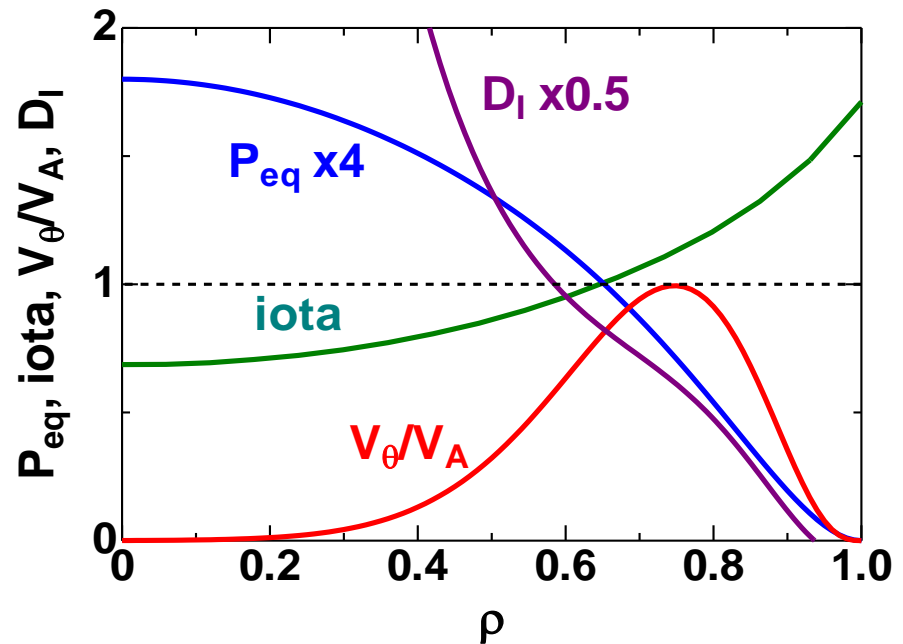
3D equilibrium



P_{eq} profile



Equilibrium pressure, rotational transform, poloidal flow, Mercier stability



$$V_A = 4.87 \times 10^6 (m/s)$$

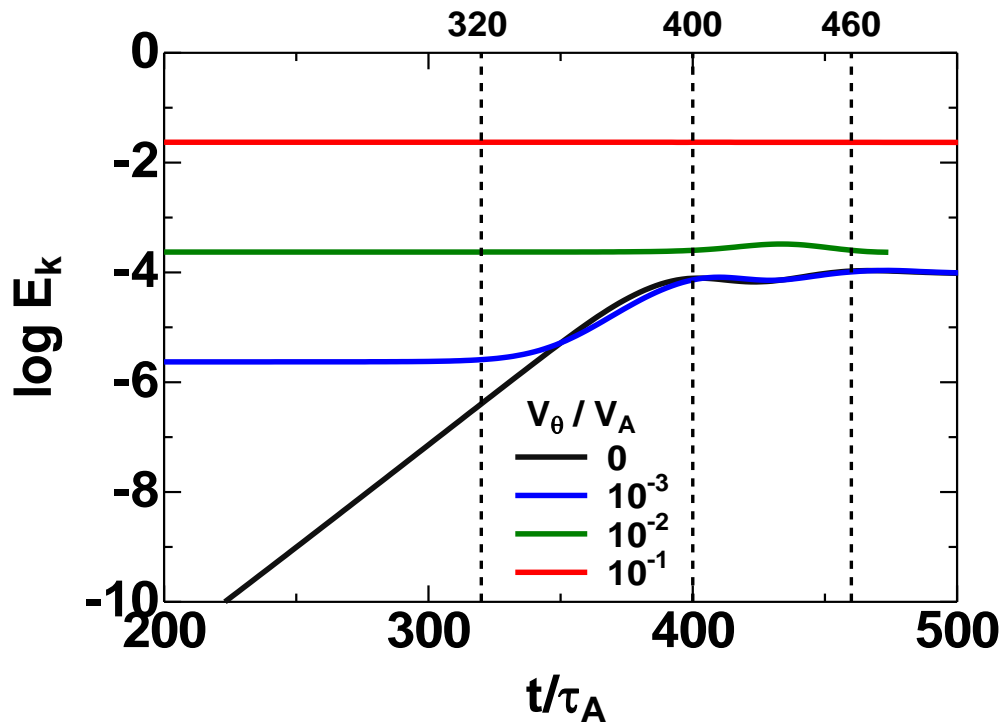
for

$$B_0 = 1(T), n_e = 0.2 \times 10^{20} (m^{-3})$$

Time evolution of pressure driven mode



● Time Evolution of kinetic energy



$$V_\theta/V_A = 0 \quad (\text{No flow})$$

After linear growth,
nonlinear saturation at $t=400\tau_A$
 $E_{\text{sat}} \sim 10^{-4}$

$$V_\theta/V_A = 10^{-3} \quad (E_k(\text{flow}) \ll E_{\text{sat}})$$

After no interaction with flow
no-flow mode dominant for $t > 340\tau_A$

$$V_\theta/V_A = 10^{-2} \quad (E_k(\text{flow}) \sim E_{\text{sat}})$$

Small interaction appears in
saturation.

$$V_\theta/V_A = 10^{-1} \quad (E_k(\text{flow}) \gg E_{\text{sat}})$$

Almost no interaction over whole
time region

Flow effects on linear mode

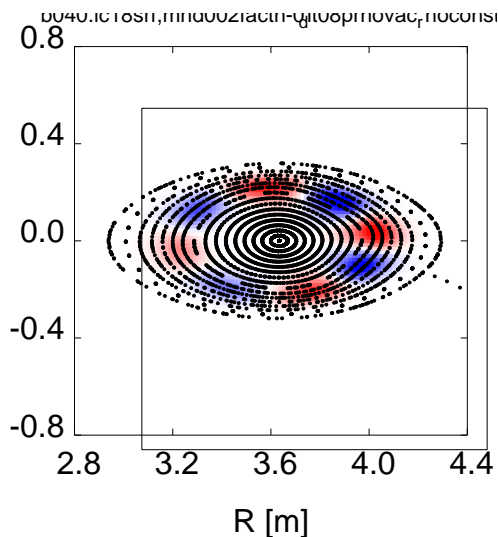


- Puncture plot and relative amplitude of perturbed pressure in linear phase

$t=320 \tau_A$

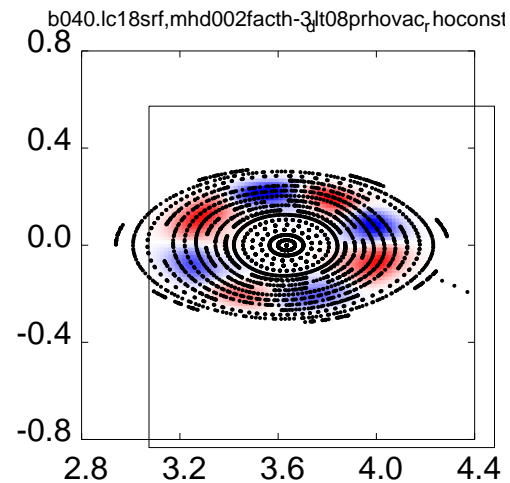
$$V_\theta/V_A = 0$$

Interchange mode with $m=4$ grows.



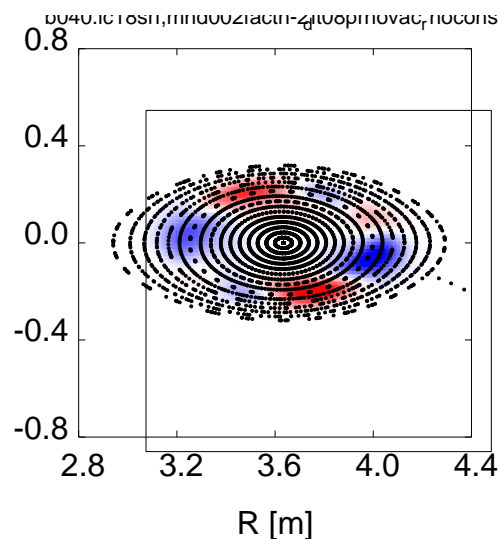
$$V_\theta/V_A = 10^{-3}$$

Almost the same as in no-flow case.



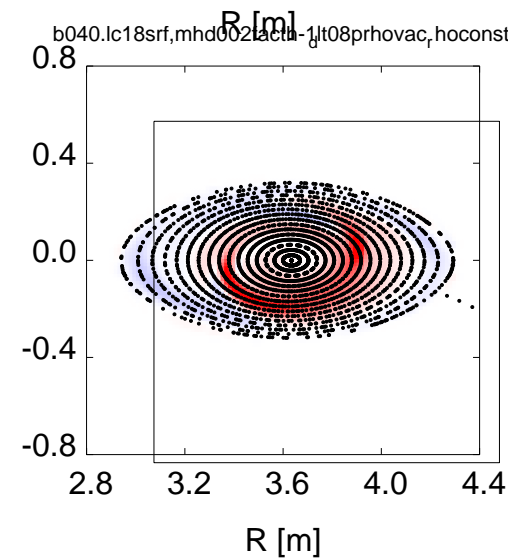
$$V_\theta/V_A = 10^{-2}$$

A mode grows but mode number is reduced to $m=2$.



$$V_\theta/V_A = 10^{-1}$$

Any mode cannot be recognized.



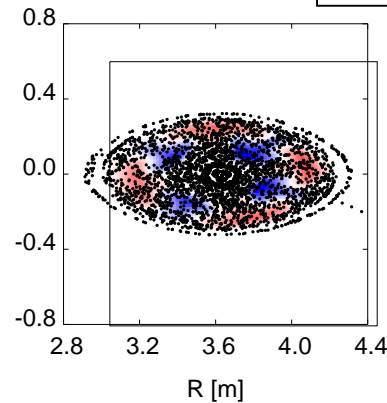
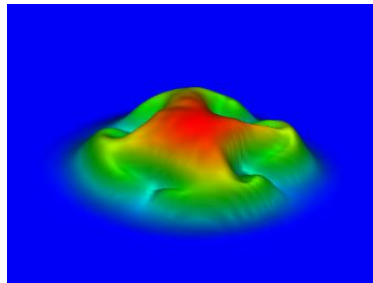
Flow dependence of nonlinear dynamics (1)



● Pressure and magnetic field lines in nonlinear saturation phase

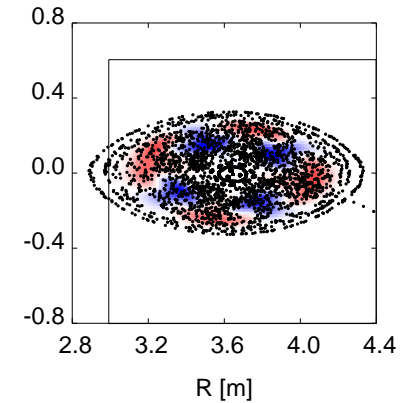
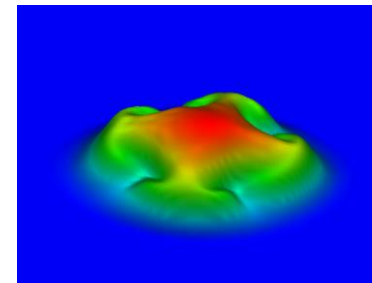
$$V_{\theta}/V_A = 0$$

$t=400 \tau_A$



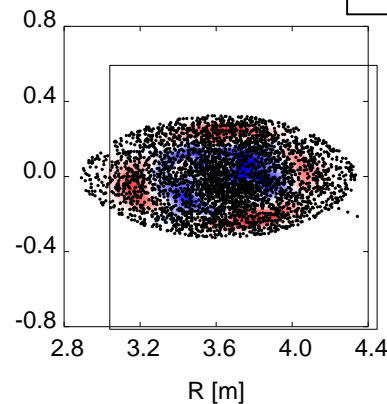
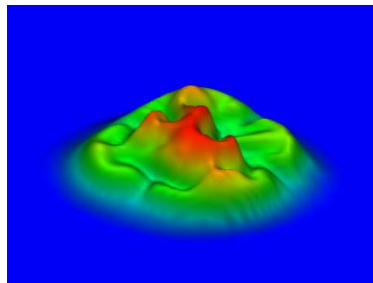
Pressure deformation with $m=4$ enhance
Core region is already stochastic.

$$V_{\theta}/V_A = 10^{-3}$$

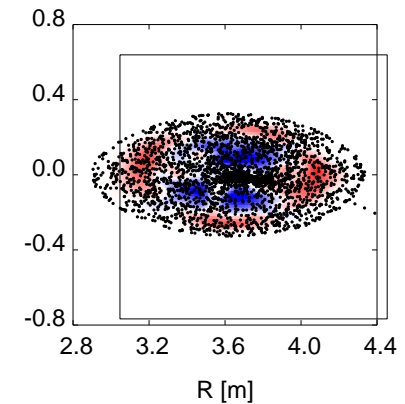
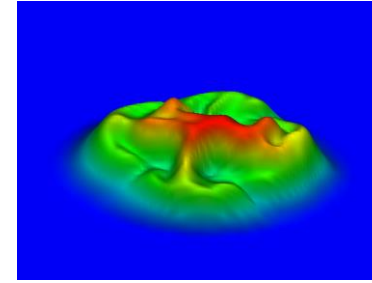


Pressure deformation and stochasticity
are similar but slightly weak.

$t=460 \tau_A$



Pressure collapses with stochastic field
lines.



Slightly weak pressure collapse
and stochastic field lines are observed.

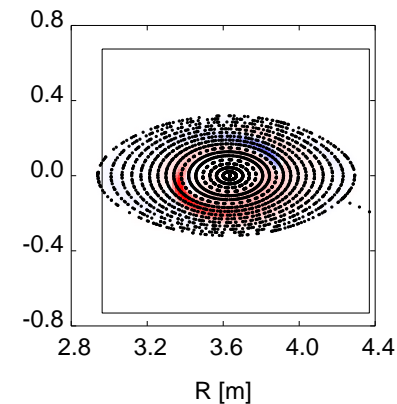
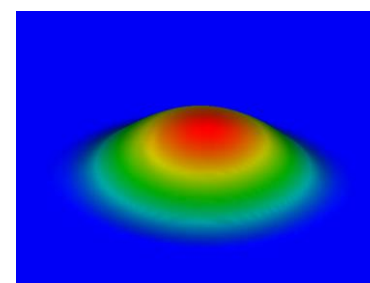
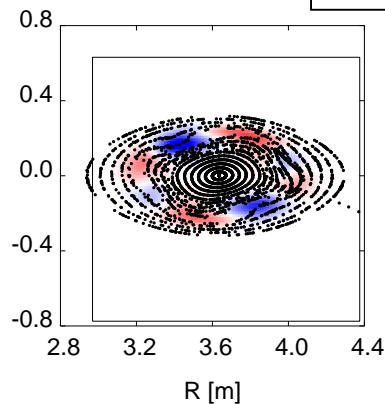
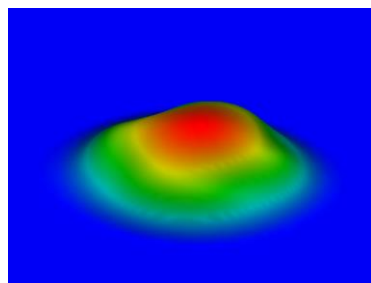
Flow dependence of nonlinear dynamics (2)



● Pressure and magnetic field lines in nonlinear saturation phase

$$V_{\theta}/V_A = 10^{-2}$$

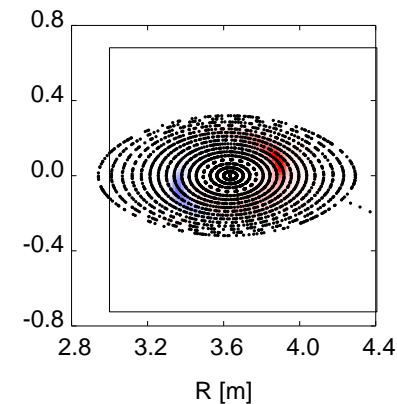
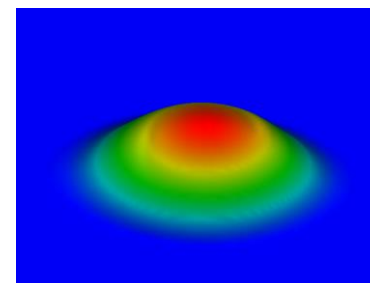
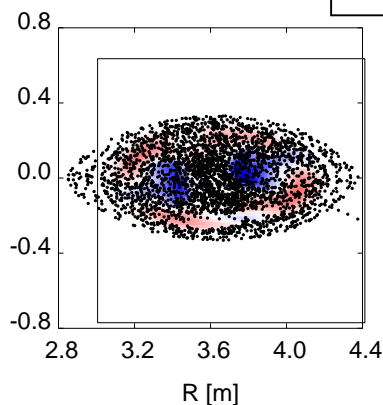
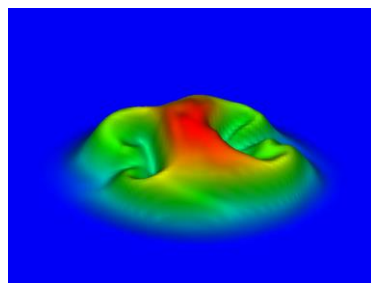
$t=400 \tau_A$



Small pressure deformation with $m=2$ appears and flux surfaces remain.

Almost no change in pressure and field lines.

$t=460 \tau_A$



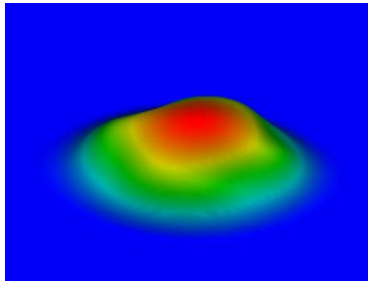
Pressure collapse and stochasticity are mitigated.

Almost no change in pressure and field lines.

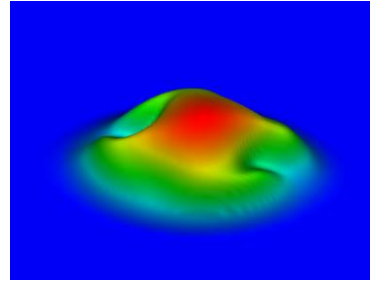
- Pressure and magnetic field lines in nonlinear saturation phase

$$V_{\theta}/V_A = 10^{-2}$$

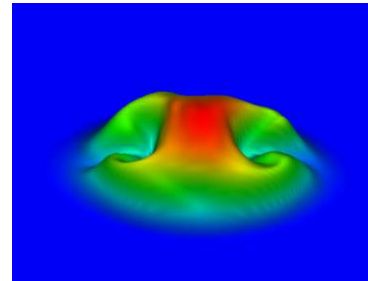
t=400 τ_A



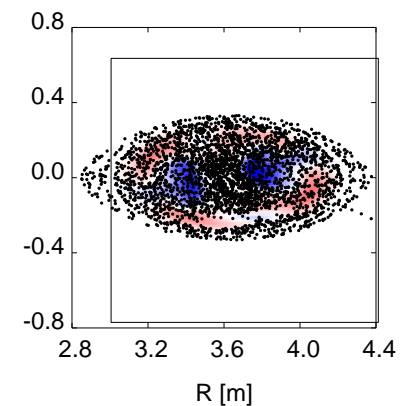
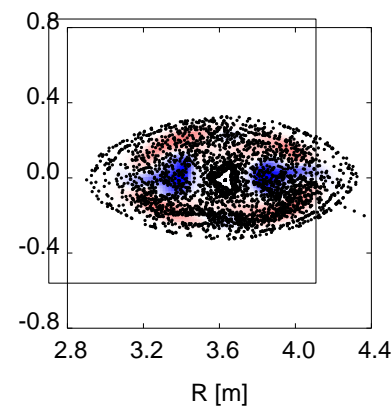
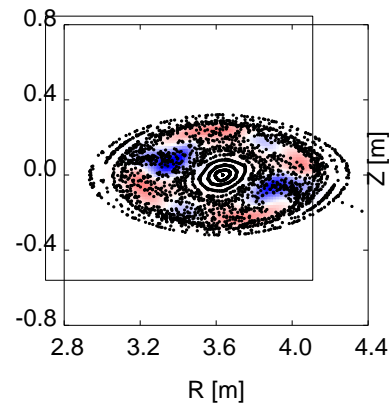
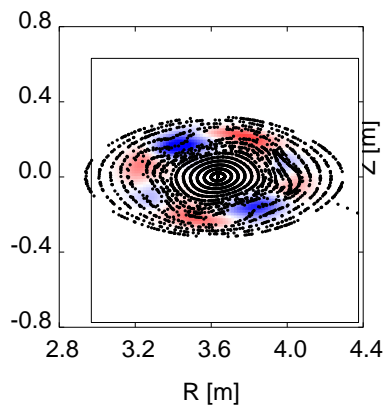
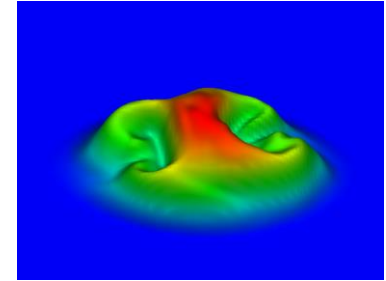
t=420 τ_A



t=440 τ_A



t=460 τ_A



Rotation of mode structure is seen.

- ◆ Effects of poloidal shear flow on the stability of interchange modes in a Large Helical Device (LHD) configuration are studied utilizing 3D numerical codes.
- ◆ Static equilibrium is employed and a model poloidal flow is incorporated as the initial perturbation.
- ◆ Stabilizing effects of the shear flow are observed :
 - No flow :
 - Growth of an interchange mode leads to pressure collapse and field line stochasticity.
 - $E_k(\text{flow}) \ll E_{\text{sat}}$:
 - Flow does not interact the mode in the linear phase and slightly weakens the collapse and stochasticity.
 - $E_k(\text{flow}) \sim E_{\text{sat}}$:
 - Flow reduces the mode number and mitigates the collapse and stochasticity with showing substantial rotation.
 - $E_k(\text{flow}) \gg E_{\text{sat}}$:
 - The mode is completely stabilized.
- ◆ More systematic analyses are necessary in future.

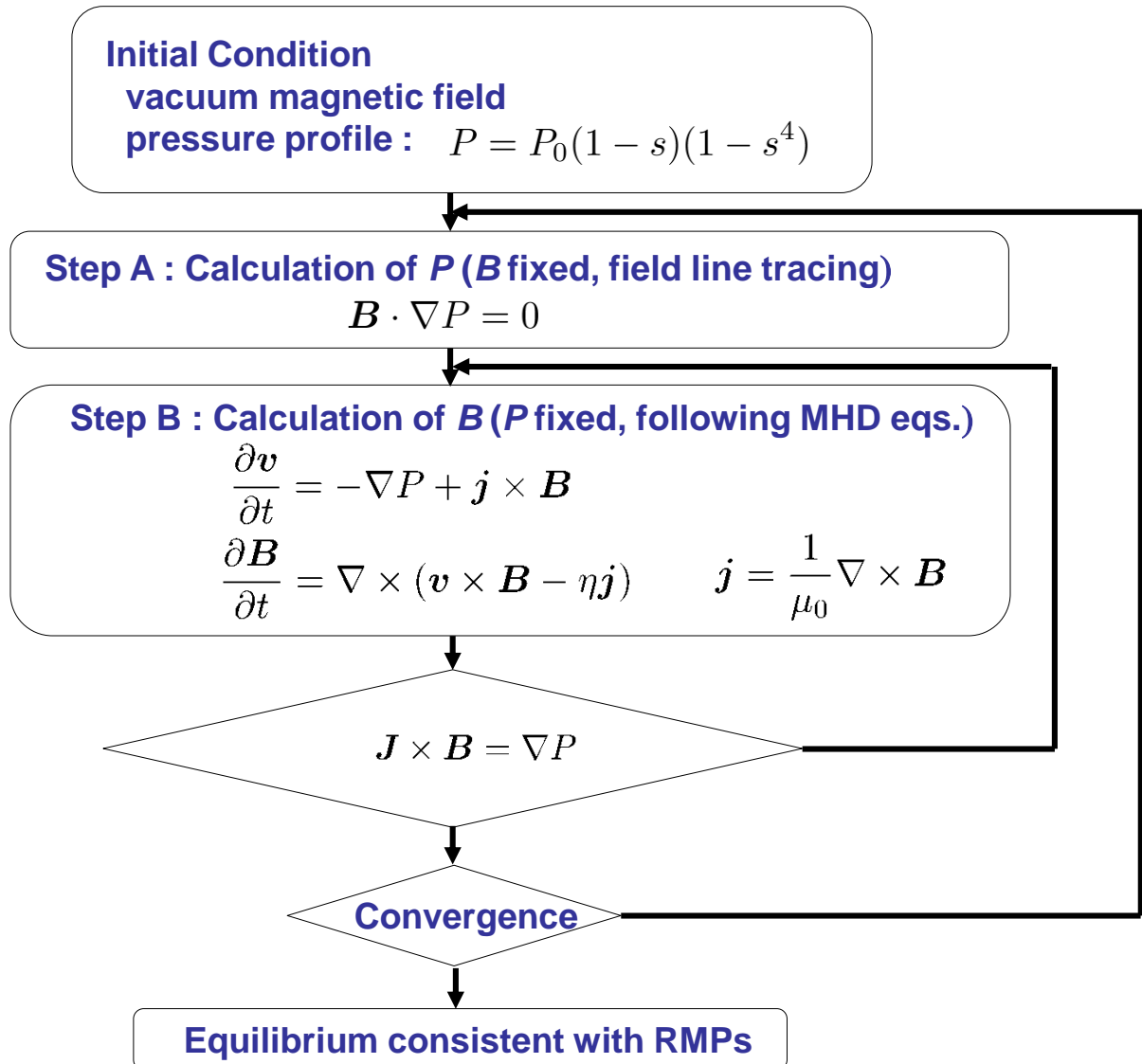
- ◆ **Stability analysis procedure of stationary state consistent with flow.**
 1. **Low beta static equilibrium is calculated with the HINT code, which is slightly unstable against interchange modes.**
 2. **With the plasma flow in the initial perturbation, the time evolution of the plasma dynamics is followed with the MIPS code.**

(Up to this point, the procedure is the same as the present case.)
 - 3, **The nonlinear saturation phase is recognized as the stationary state consistent with the flow, which is stable for the interchange modes.**
 4. **The stability of the stationary state is examined against the perturbation generated by the change of equilibrium quantity.**
 - a. **beta ramp up with heat source term**
 - b. **rotational transform change with increasing net current**

● HINT2 code

(Y. Suzuki, et al.,
Nuclear Fusion (2006) L19)

- The HINT2 code solves the 3D equilibrium equations without any assumptions of the existence of the nested flux surfaces. (suitable for the equilibrium analysis including RMPs)
- An LHD configuration with an inwardly shifted vacuum magnetic axis and a high aspect ration is employed. (Rax=3.6m, $\gamma=1.13$)
- Calculation starts with the parabolic pressure profile with $\beta_0 = 4.4\%$.



- **MIPS code** (Todo et al., Plasma Fus. Res. (2010) S2062)
Solves the full MHD equations by following the time evolution.
4th order central difference method for (R, ϕ , Z) directions.
4th order Runge Kutta scheme for the time evolution.
The most unstable mode is detected.

Basic equations

$$\frac{\partial \rho}{\partial t} = -\nabla \cdot (\rho \mathbf{v})$$

$$\begin{aligned} \frac{\partial \mathbf{v}}{\partial t} = & -\rho \mathbf{w} \times \mathbf{v} - \rho \nabla \left(\frac{v^2}{2} \right) - \nabla p + \mathbf{j} \times \mathbf{B} \\ & + \frac{3}{4} \nabla [\nu \rho (\nabla \cdot \mathbf{v})] - \nabla \times (\nu \rho \mathbf{w}) \end{aligned}$$

$$\frac{\partial \mathbf{B}}{\partial t} = -\nabla \times \mathbf{E}$$

$$\frac{\partial p}{\partial t} = -\nabla \cdot (p \mathbf{v}) - (\Gamma - 1) p \nabla \cdot \mathbf{v} + \chi_{\perp} \nabla_{\perp}^2 (p - p_{eq}) + \chi_{\parallel} \nabla_{\parallel}^2 p$$

$$\mathbf{E} = -\mathbf{v} \times \mathbf{B} + \eta (\mathbf{j} - \mathbf{j}_{eq})$$

$$\mathbf{J} = \frac{1}{\mu_0} \nabla \times \mathbf{B}$$

$$\mathbf{w} = \nabla \times \mathbf{v}$$